TISSUE ENGINEERING: Part A
Volume 19, Numbers 9 and 10, 2013

DOI: 10.1089/ten.tea.2012.0321

# Engineering Cellular Fibers for Musculoskeletal Soft Tissues Using Directed Self-Assembly

Nathan R. Schiele, MS,[1] Ryan A. Koppes, MS,[1] Douglas B. Chrisey, PhD,[2] and David T. Corr, PhD[1]

Engineering strategies guided by developmental biology may enhance and accelerate *in vitro* tissue formation for tissue engineering and regenerative medicine applications. In this study, we looked toward embryonic tendon development as a model system to guide our soft tissue engineering approach. To direct cellular self-assembly, we utilized laser micromachined, differentially adherent growth channels lined with fibronectin. The micromachined growth channels directed human dermal fibroblast cells to form single cellular fibers, without the need for a provisional three-dimensional extracellular matrix or scaffold to establish a fiber structure. Therefore, the resulting tissue structure and mechanical characteristics were determined solely by the cells. Due to the self-assembly nature of this approach, the growing fibers exhibit some key aspects of embryonic tendon development, such as high cellularity, the rapid formation (within 24 h) of a highly organized and aligned cellular structure, and the expression of cadherin-11 (indicating direct cell-to-cell adhesions). To provide a dynamic mechanical environment, we have also developed and characterized a method to apply precise cyclic tensile strain to the cellular fibers as they develop. After an initial period of cellular fiber formation (24 h postseeding), cyclic strain was applied for 48 h, in 8-h intervals, with tensile strain increasing from 0.7% to 1.0%, and at a frequency of 0.5 Hz. Dynamic loading dramatically increased cellular fiber mechanical properties with a nearly twofold increase in both the linear region stiffness and maximum load at failure, thereby demonstrating a mechanism for enhancing cellular fiber formation and mechanical properties. Tissue engineering strategies, designed to capture key aspects of embryonic development, may provide unique insight into accelerated maturation of engineered replacement tissue, and offer significant advances for regenerative medicine applications in tendon, ligament, and other fibrous soft tissues.

## Introduction

Tendons and ligaments are dense, collagen-based, tissues that transmit mechanical forces and stabilize joints, allowing for basic human functions and locomotion. The hierarchical tendon and ligament structure is composed of fascicles, made up of collagen fibers. These collagen fibers are formed from continuous collagen fibrils, aligned to the tissue long-axis to provide the mechanical strength.[1] The high incidence of injury and poor intrinsic healing of these tissues make them attractive candidates for tissue engineering and regenerative medicine.[2]

Cell-based tissue engineering presents a unique approach to *in vitro* tissue formation by exploiting the fundamental ability of cells to self-organize and synthesize their own extracellular matrix (ECM) proteins. Current scaffold-free and cell-based engineering methodologies have produced tendon and ligament-like structures from two-dimensional (2D) cell monolayers cultured in dishes. Human connective tissue progenitor cells,[3] tendon fibroblasts,[4–6] and bone marrow stromal cells,[7] have been grown in monolayer culture and allowed to contract, or roll-up, to form three-dimensional (3D), fiber-like structures. Using an alternative scaffold-free approach, de Wreede and Ralphs[8] cultured a suspension of tendon fibroblasts in a rotating dialysis tube for 14 days to produce fiber-like cell aggregates. Although successful at producing tissue, these previous scaffold-free and cell-based techniques are unable to precisely control the cellular organization and final tissue structure. To provide additional signals for cellular organization and alignment in culture, Patz *et al.*[9] utilized differentially adherent growth channels, filled with a basement membrane matrix (Matrigel™), to direct the aligned growth of mouse C2C12 myoblast cells. While these results showed promise for guiding myoblast growth, the Matrigel within the growth channels fills the volumetric space potentially limiting cell-to-cell adhesion

[1]Biomedical Engineering Department, Rensselaer Polytechnic Institute, Troy, New York.
[2]Department of Physics and Engineering Physics, Tulane University, New Orleans, Los Angeles.

early in development, establishes a non-native provisional scaffold, and introduces unintended and uncontrolled growth factors and ECM components.[10,11]

It has been recently suggested that looking toward embryonic tendon development for guidance may provide strategies to improve functional outcomes, in both regenerative medicine and tissue engineering applications.[12,13] In stark contrast to the dense collagen ECM found in mature tendons and ligaments, developing tissues are characterized by a low collagen content and high cellularity, especially at the early stages of embryonic development.[14] As seen in developing rabbit flexor tendons and postnatal mouse Achilles tendons, developing tendons are highly cellular with a low total collagen content (~3% collagen at 4 days postnatal and ~36% at 28 days) when compared to mature tendons.[15,16] Electron microscopy of the embryonic human flexor tendon revealed the presence of direct cell-to-cell adhesions that remain throughout differentiation, and suggested these direct cellular connections allow for external force transmission in the developing tendon during embryogenesis.[17] Even with maturity, tendon cells maintain cell-to-cell contact through gap junctions, and these junctions may play a role in producing a coordinated cellular response to mechanical loading.[18] In the embryonic tendon, the tightly packed and aligned cells that form the tendon structure are in direct cell-to-cell contact, mediated by cadherin-11,[19] a homophilic cell-to-cell adhesion protein.[20] Cadherin-11-mediated cell-to-cell adhesions were found to be essential for the formation of the organized collagen network in a developing tendon.[19]

Strong cell-to-cell adhesion may be required throughout embryonic and postnatal development, as movements driven by muscle contraction require force transmission through the highly cellular developing tendons, even before the ECM network has reached maturity. Embryos display spontaneous movements, as early as embryonic day 12.5 in mouse,[21] and day 3 in chick,[22] resulting in a dynamic mechanical environment.

Looking toward embryonic development for guidance and using embryonic tendon as a model system to educate our approach, we have developed a cell-based method to engineer single cellular fibers for musculoskeletal soft tissues. Reminiscent of the highly cellular early stages of the embryonic tendon, we have created a highly cellular microenvironment that directs cell alignment and exploits the intrinsic ability of cells to self-assemble through cell-to-cell adhesions to form single fibers. This cellular, single-fiber approach employs laser micromachined, differentially adherent growth channels coated with fibronectin, a protein found in tendon during the early stages of embryonic development.[23] To represent the dynamic mechanical embryonic environment, we have created a method to apply a well-characterized cyclic tensile strain to the cellular fibers as they develop. Human dermal fibroblasts, cells utilized clinically for tendon healing, and tissue-engineered tendon,[24–26] were used to evaluate the cellular fiber structure and the effect of cyclic strain on mechanical properties. This cellular fiber tissue engineering approach could provide the foundation for soft tissue replacements (e.g., tendon and ligament) as well as an *in vitro* test bench for investigating embryonic-inspired biophysical factors (e.g., mechanical cues and soluble factors).

## Materials and Methods

### *Growth channel fabrication*

A 2-wt% concentration of agarose gel was prepared by mixing 1.0 g of electrophoresis-grade agarose powder (Invitrogen, Carlsbad, CA) with 50 mL of Dulbecco's modified Eagle's medium (DMEM). Once heated to ~80°C, 6.0 mL of the liquid agarose was pipetted into 47-mm-diameter Petri dishes. After cooling and gelation, the agarose-filled Petri dishes were mounted on an x-y motorized, computer-controlled stage. A pulsed excimer laser ($\lambda = 193$ nm; TeoSys, Crofton, MD) with computer-aided design (CAD)/computer-aided manufacturing control was used to micromachine 3D growth channels into the agarose gel. Growth channel dimensions were specified in a CAD software package, and converted to laser firing and motion control code. The 3D growth channels were micromachined to a length of 1.65 cm (Fig. 1a), width at the surface of the agarose of ~250 μm, and a depth of ~300 μm (Fig. 1c).

### *Growth channel assembly*

Human plasma-derived fibronectin (BD Biosciences, Bedford, MA) was diluted to 1 mg/mL in sterile cell culture grade water, and further reduced to 0.375 mg/mL in DMEM. Fibronectin (30 μL) was flowed into the growth channel, and then dried, creating a differentially adherent growth channel. To provide anchor points for the developing fibers, collagen sponge disks were incorporated into each end of the growth channel (Fig. 1b). Two, 4-mm-diameter disks were cut from sterile fibrous collagen sponge pads (Bovine Type I; Kensey Nash Corp., Exton, PA) using a biopsy punch, and then inserted into corresponding 4-mm-diameter cut-outs created in the agarose.


**FIG. 1.** **(a)** Top view of a growth channel laser micromachined into agarose gel, demonstrating consistent dimensions along its 1.65-cm length. **(b)** Two 4-mm-diameter collagen sponge disks are inserted into each end of the growth channel to act as anchor points for the developing cellular fiber. **(c)** A cross section of growth channel demonstrates its depth and three-dimensional structure.

Flexcell® (Flexcell International Inc., Hillsborough, NC), Tissue Train® plates were modified to include vertical loading posts (17-gauge, stainless steel) affixed to each of the Tissue Train plate nylon tabs. The agarose surrounding the growth channel was trimmed to uniform rectangular (2.7-cm length and 1-cm width) specimens. The growth channel was removed from the Petri dish and mounted on the loading posts of the modified Tissue Train plate, and then coupled to the plate through 1 mm diameter centered through holes in the collagen sponge disks (Fig. 2b). Coupling the growth channel assembly to the Tissue Train plates allows dynamic, uniaxial cyclic strain to be applied to the developing fibers.

### *Digital image correlation for strain characterization*

To determine the precise amount of strain experienced by the developing fibers, the cyclic tensile strain applied directly to the growth channels through the modified Tissue Train plates was characterized. The growth channels were prepared and assembled as described (coated with fibronectin, dried, filled with culture media, and stored in a standard cell culture incubator for 24 h). The top surface of the growth channel was blotted dry and coated with an anisotropic, high-contrast speckle pattern, and mounted onto a modified Tissue Train plate containing 1 mL of DMEM warmed to 37°C (to replicate normal culture conditions) (Fig. 2b). Cyclic tensile strain was applied using the Flexcell system via the computer-controlled vacuum pump and deformable membrane in the Tissue Train plate. The strain magnitude was specified in the Flexcell software to be 0.7% and 1.0% strain, with each magnitude cycled two times at a frequency of 0.1 Hz using a sine waveform ($n=10$ separate growth channel assemblies). The system was also calibrated for applied strains of 0.7%, 0.75%, 1.0%, 1.5%, and 2.0% (five cycles each at 0.5 Hz, $n=7$ separate growth channels). Two cameras of a digital image correlation system were mounted on a tripod over the growth channels (Fig. 2a) and calibrated using calibration grids (Correlated Solutions, Inc., Columbia, SC). Video of the strained growth channels were collected at 10 frames per second, and the noncontacting strain analysis was completed using VIC-3D 2010 digital image correlation software (Correlated Solutions, Inc.). A virtual extensometer was placed in-line with the growth channel to calculate the magnitude of cyclic tensile strain experienced by the developing fibers in the growth channel. Data are reported as the mean peak strain ± standard deviation (%).

### *Cell culture*

Neonatal human dermal fibroblasts (ATCC, Manassas, VA) were grown in T-75-$cm^2$ tissue culture flasks using a standard growth medium. Cells were lifted from flasks with trypsin, centrifuged, and resuspended in the culture medium (DMEM, supplemented with 10% fetal bovine serum, 0.5% penicillin–streptomycin, and 50 μg/mL L-ascorbic acid). A cell suspension containing $2\times10^5$ cells/mL was pipetted into the fibronectin-coated, agarose growth channels, and fresh culture medium was added 5 min after seeding. The growth channels were then placed into a standard cell culture incubator (37°C, 5% $CO_2$, 95% relative humidity) and the culture medium was exchanged after 24 h.

### *Immunocytochemistry for cadherin-11*

Fibers were fixed in the growth channels with 4% paraformaldehyde for 1 h at room temperature, at 4, 24, and 72 h of development. Following three rinses with phosphate-

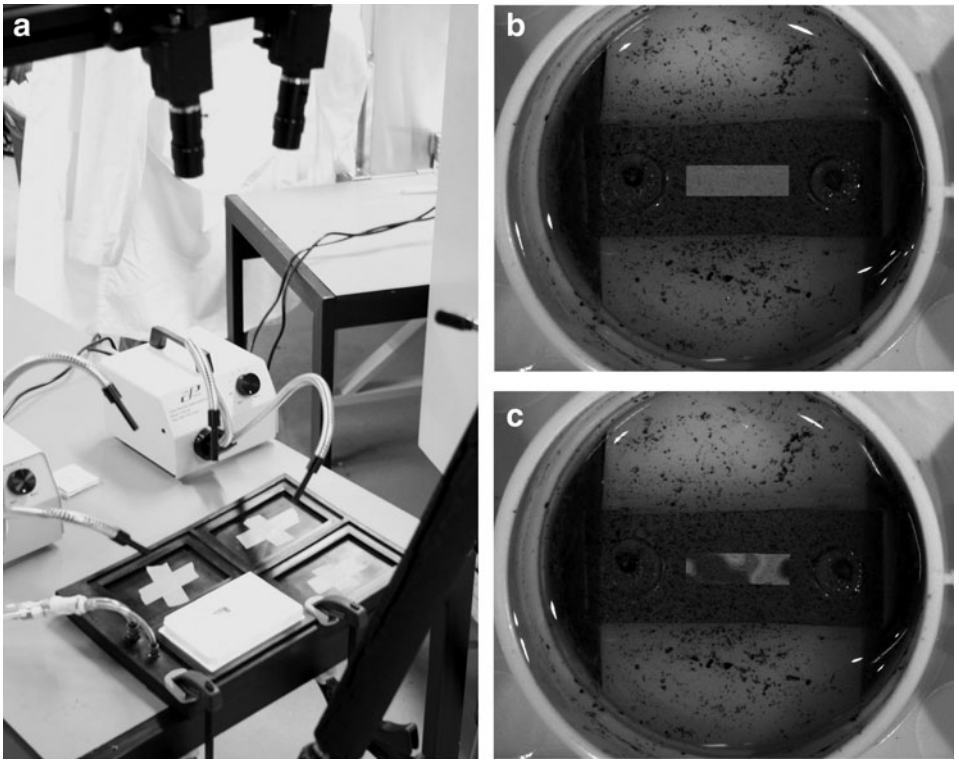


**FIG. 2.** Noncontacting calibration of strain in the growth channel assemblies mounted in modified Flexcell Tissue Train plates. **(a)** A two-camera digital image correlation system is mounted above the Flexcell plate to capture video, while the growth channel assemblies are cyclically strained. **(b)** An unstrained growth channel assembly, mounted onto the modified Tissue Train plate, coated with a high-contrast speckle pattern and area of interest selected for digital image correlation and strain calculations, and **(c)** a growth channel assembly cyclically strained by the Flexcell system.

buffered saline (PBS), fibers were permeabilized with 0.5% Triton X-100 for 30 min, and then blocked in 2% bovine serum albumin (BSA) in PBST (PBS with 0.8% Tween 20) for 1 h. The primary rabbit antibody for cadherin-11 (Invitrogen) was diluted (1:100) in 2% BSA in PBST and incubated for 1 h at room temperature. Following three washes with PBST, the fibers were incubated with the FITC-conjugated goat anti-rabbit secondary antibody (1:1000) for 1 h at room temperature. Hoechst (Invitrogen) was used to stain cell nuclei. Following three washes with PBST, the fibers were removed from the channels, mounted on slides with the fluoro-gel mounting medium (Electron Microscopy Services, Hatfield, PA) and sealed with coverslips. Staining was conducted in triplicate, and control fibers with the primary antibody omitted showed minimal background fluorescence.

### *Fast Fourier transform image analysis for cellular organization*

The time course of cellular organization within the developing fibers (at 4, 24, and 72 h of development) was investigated using the fluorescently stained cell nuclei. A fast Fourier transform (FFT) analysis was utilized, similar to that previously used to quantify the alignment of various structures, such as collagen fibers, cell nuclei, and f-actin.[27–29] A custom MATLAB (The MathWorks, Inc., Natick, MA) program was developed to perform 2D FFT analysis on the images ($n = 3$ for each time point) of Hoechst-stained cell nuclei within the fibers, and to produce plots of power spectrum intensity and corresponding histograms of the intensity distribution (Fig. 3). Grayscale images were first converted to binary and windowed with a Gaussian profile to reduce edge effects.[28,30] To quantify the cellular organization in the developing fibers, an alignment index was assigned based on the fraction of intensities within 20° of the peak angle, as seen from the intensity distribution histogram.[27,29] A higher alignment index indicates a larger number of cells aligned to the same direction, and thus, less angular dispersion and greater alignment.

### *Dynamic mechanical stimulation of single cellular fibers*

Following 24 h of static growth (0% applied strain), initial cellular fiber formation and integration into both collagen disks was verified using an optical microscope. Cellular fibers were then subjected to a 48-h regimen of intermittent cyclic tensile strain using the modified and characterized Flexcell system. The loading protocol consisted of six, 8-h blocks, alternating 8 h of cyclic strain at 0.5 Hz with 8 h of static tension (0% applied strain): 8 h of 0.7% applied cyclic strain, 8 h of static, 8 h of 0.75% cyclic strain, 8 h static, 8 h of 1.0% cyclic strain, 8 h of static, for a total time in culture of 72 h (Fig. 4). The applied strain magnitudes were within normal physiological strain experienced by the mature tendon.[31] Static tension controls (0% applied strain) were conducted using identical growth channel assemblies, mounted in the modified Tissue Train plates and seeded with cells, but not subjected to dynamic strain by the Flexcell system.

### *Mechanical evaluation of single cellular fibers*

Following 72 h in culture, which included 24 h of static growth and three 8-h intervals of cyclic tensile strain, cellular fibers were removed from the growth channels and placed in a PBS bath. Cellular fibers were sectioned into test specimens with a ~150-μm gauge length. While submerged in PBS, each fiber section was secured at both ends using laser-cut aluminum T-clips (MicroConnex, Snoqualmie, WA) to grip the fiber (Fig. 5). The T-clipped fiber sections were then mounted for mechanical evaluation in a PBS-filled bath of a custom microscope-based single fiber mechanics rig.[32] Load was measured using a force gauge, AE-800 Series sensor element (SensorOne Technologies Corp., Sausalito, CA), and displacement with a digital micrometer. Each fiber specimen was uniaxially elongated in tension to failure using the rig's micrometer/micromanipulator. Data are reported as mean ± standard deviation.

### *Statistical analysis*

Differences in growth channel strain magnitudes (determined from digital image correlation), comparisons of alignment index (determined from FFT image analysis) between each time point, and differences in maximum force, displacement at maximum force, and linear-region stiffness between static tension control fibers and cyclically strained fibers were assessed using two-tailed, unpaired Student's *t*-tests with a level of $p < 0.05$ to establish statistical significance.

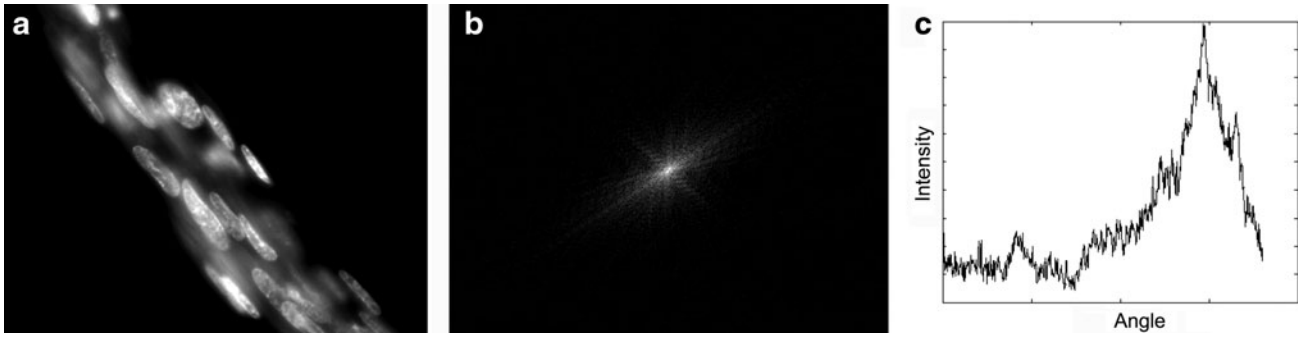


**FIG. 3.** **(a)** Original image of cell nuclei (Hoechst) in a fiber following 72 h of development. **(b)** The power spectrum obtained from the fast Fourier transform analysis of the cell nuclei, and **(c)** the resulting intensity frequency distribution plotted from the power spectrum.

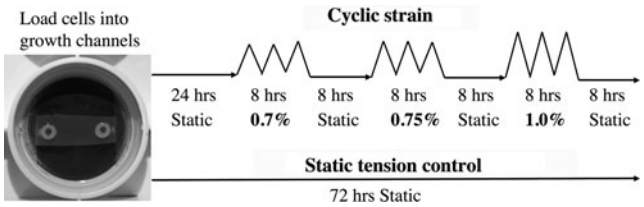


**FIG. 4.** Schematic of the dynamic stimulation protocol. Developing fibers were allowed 24 h of static growth (0% applied strain) before the application of three intermittent, 8-h intervals of increasing cyclic strain (0.7%, 0.75%, and 1.0% applied at 0.5 Hz). Static tension controls were grown identically, but no cyclic strain was applied.

## Results

The fibronectin-coated, laser micromachined, agarose growth channels provided a differentially adherent substrate that directed fibroblast cells to organize and self-assemble into single cellular fibers. The cellular fibers formed rapidly, within 24 h, and became well integrated into the collagen sponge disk anchor points at both ends of the channels (Fig. 6). The fibers develop considerable self-generated static tension within 24 h, as evidenced by a rapid retraction of the free fiber ends toward the anchor points following complete transection of the fiber midsubstance (not shown).


**FIG. 5.** A cellular fiber test section gripped with T-clips for mechanical evaluation on a custom microscope-based, single-fiber mechanics rig.

### *Cadherin-11 expression*

Cadherin-11 was detected in the cellular fibers at all time intervals using immunocytochemistry. The punctate distribution of cadherin-11 expressed throughout the fiber within 24 h of development (Fig. 7) indicates direct cell-to-cell adhesions in the developing cellular fibers.

### *Cellular organization in developing cellular fibers*

The fibers appeared to be highly cellular at all time points (Fig. 8). Organization of the cells within the developing fibers was evaluated using FFT analysis of cell nuclei, and quantified using an alignment index. At 4 h, the cells had the lowest alignment index, indicating a greater angular dispersion and less organization. The cells became more organized, with significant increases in alignment index following 24 h ($p=0.014$) and 72 h ($p=0.011$) of development, compared to 4 h (Fig. 8). No significant change in cell nuclei alignment was observed from 24 to 72 h ($p=0.20$), indicating that the organization achieved at 24 h was maintained at 72 h.

### *Strain characterization*

The modified Flexcell Tissue Train plates can apply cyclic tensile strain to the developing cellular fibers in the agarose growth channel assemblies (Fig. 9). When operating at a frequency of 0.1 Hz and a strain magnitude of 0.7%, as specified in the Flexcell software, the growth channels are subjected to $0.79\% \pm 0.1\%$ strain, determined from digital image correlation. When a 1.0% strain at 0.1 Hz was specified, the growth channels strained $1.22\% \pm 0.13\%$ (Table 1). At 0.1 Hz, the specified 0.7% strain produced strains in the growth channels significantly different ($p=0.002$) than 1.0% strain. The frequency of peak strain in the growth channels matches the specified waveform frequency (0.1 Hz), with peak strains occurring once every $10 \pm 0.1$ s ($n=20$). The system was also calibrated for a frequency of 0.5 Hz (Fig. 9). The growth channels strained $0.77\% \pm 0.12\%$, $0.83\% \pm 0.12\%$, $1.21\% \pm 0.17\%$, $1.49\% \pm 0.21\%$, and $1.6\% \pm 0.21\%$ for each Flexcell specified strain of 0.7%, 0.75%, 1.0%, 1.5%, and 2.0%, respectively (Table 1). Peak strains occurred once every $2 \pm 0.1$ s ($n=20$), matching the desired 0.5 Hz frequency.

The waveform frequency does not alter the ability of the system to apply a predictable strain to the developing fibers. When 0.7% strain at 0.1 Hz was specified, there was no difference ($p=0.35$) in the strain experienced by the growth channel when strained at 0.7% and 0.5 Hz. Likewise, there was no difference ($p=0.72$) in the growth channel strain between 1.0% strain at 0.1 Hz and 1.0% strain at 0.5 Hz. These results support our ability to apply dynamic strains of precise magnitudes at desired frequencies, to the fibers during development.

### *Mechanical evaluation*

Following 72 h of development, cellular fibers subjected to either static growth (0% applied strain) ($n=6$) or the cyclic strain protocol ($n=5$), were removed from the growth channels intact using tweezers, T-clipped, and mounted onto the single-fiber mechanics rig for mechanical evaluation. This indicates a basal level of mechanical stability was achieved within 72 h. Fiber dimensions, measured using a stereoscope

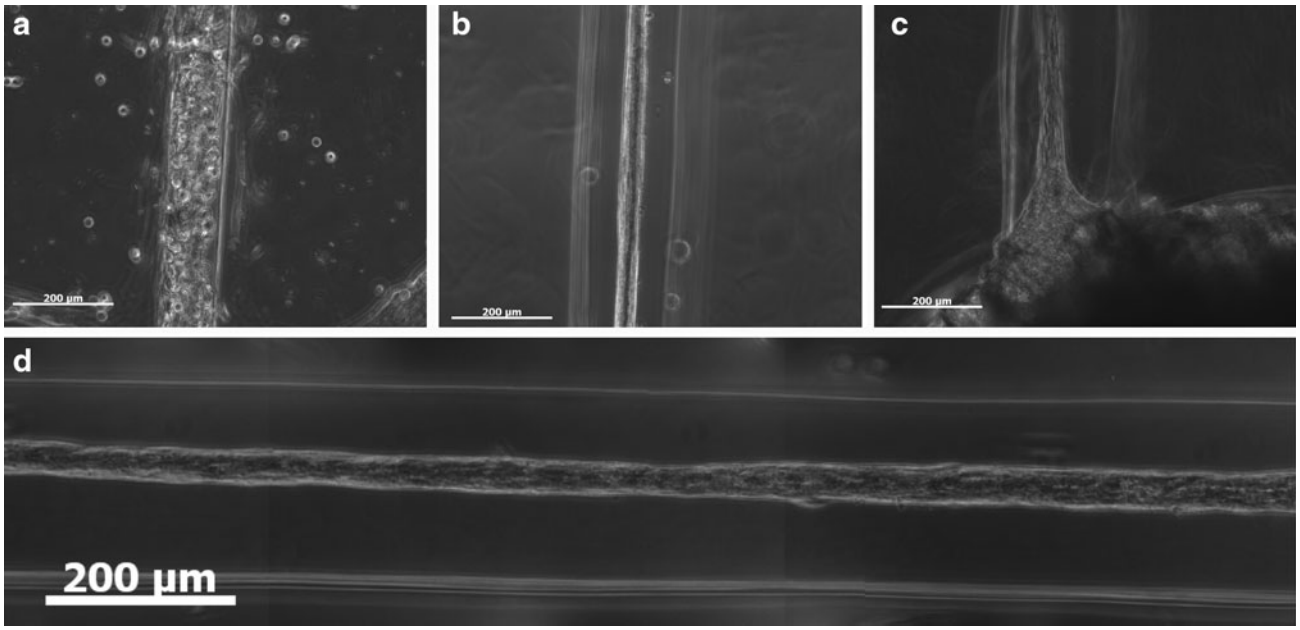


**FIG. 6.** Representative phase-contrast images of fiber development throughout the first 72 h. **(a)** At 4 h following seeding the growth channel with fibroblasts, the channel appears highly cellular and individual cells are readily identified. The fibronectin-coated growth channel and surrounding agarose provides a differentially adherent substrate where cells adhere within the growth channel, but not to the surrounding agarose. **(b)** By 24 h of development, the cells grow together and form a single cellular fiber, and **(c)** the fiber becomes well integrated to the collagen sponge anchor points at each end of the growth channel. The resulting cellular fiber is continuous between the anchor points along the 1.65 cm length of the growth channel. **(d)** At 72 h of development, fiber continuity and stability is maintained.

and camera system on the mechanics rig, showed no difference in the cross-sectional area between static or cyclically strained fibers ($p = 0.29$). The maximum force (ultimate force) of the cyclically strained cellular fibers ($0.07 \pm 0.02$ mN) was significantly larger compared with the static control fibers ($0.04 \pm 0.01$ mN) ($p = 0.017$; Table 2). Similarly, the cyclically strained cellular fibers had a significantly larger displacement at the maximum force ($0.84 \pm 0.17$ mm) compared to the static control fibers ($0.52 \pm 0.17$ mm) ($p = 0.012$; Table 2).

The linear-region stiffness was determined from the slope of a line fit to the force–displacement curve that achieved a $R^2 > 0.90$. Cyclically strained cellular fibers had a greater linear-region stiffness ($0.18 \pm 0.07$ mN/mm) than static control fibers ($0.1 \pm 0.03$ mN/mm) (Table 2). This nearly twofold increase in the linear-region stiffness approached statistical significance ($p = 0.06$).

## Discussion

Embryonic tendon development provides a functional example of cellular self-assembly, organization, and tissue formation. While all aspects of embryonic development cannot be mimicked *in vitro*, incorporating some key aspects characteristic of early tenogenesis, such as high cellularity, a reduced exogenous protein microenvironment, an organized structure of cells in direct cell-to-cell contact, and a dynamic mechanical environment, may prove beneficial to realizing functional cell-based soft tissue engineering.

In an effort to capture a few key aspects of early embryonic development, we have demonstrated a cell-based approach utilizing differentially adherent growth channels to direct cells to self-assemble into single fibers. The resulting cellular fibers had an organized 3D structure of cells in direct

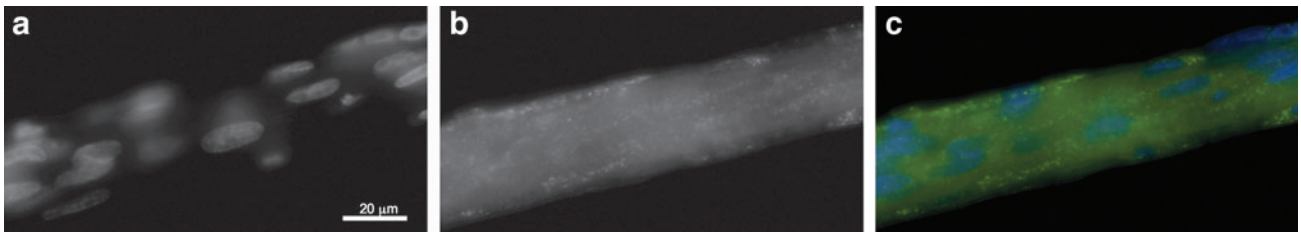


**FIG. 7.** Representative immunofluorescence image of a cellular fiber at 24 h of development identifying the **(a)** cell nuclei and **(b)** the expression of cadherin-11. The bright punctate stain distribution of cadherin-11 is clearly visible throughout the highly cellular fiber structure in **(c)** the merged image of cell nuclei (blue) and cadherin-11 (green). Color images available online at www.liebertpub.com/tea

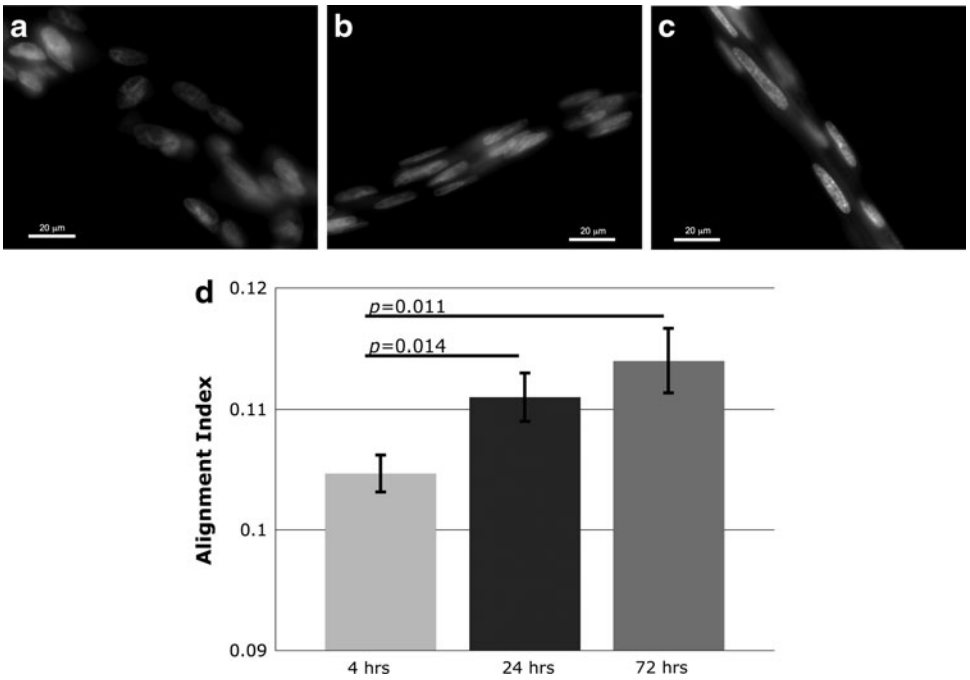


**FIG. 8.** Representative images of cell nuclei within developing fibers at **(a)** 4, **(b)** 24, and **(c)** 72 h. The fibers appear highly cellular at all time points, and increasing in organization and alignment with time. Cell nuclei seen above and below the plane of focus indicate a three-dimensional fibrous structure. **(d)** The alignment index shows that cells organize rapidly in the developing fibers; the significant increase in cellular organization seen at 24 h is maintained at 72 h ($p = 0.20$).

cell-to-cell contact. To mimic the dynamic embryonic mechanical environment, we applied a well-characterized cyclic strain to the fibers, while they developed.

Micromachined growth channels provide a controlled microenvironment that rapidly (within 24 h) guided cellular organization to form single fibers and encouraged cell-to-cell adhesion, as indicated by the expression of the cell-to-cell adhesion protein, cadherin-11. This is reminiscent of embryonic tendon; in which cadherin-11 is highly expressed and directly adheres adjacent cells.[19] The presence of cadherin-11 in our engineered fibers suggests that cell-to-cell adhesion may play a critical role in cellular self-assembly and fiber formation. Future work will investigate the role that cadherin-11 and direct cell-to-cell adhesions play in tissue formation, and how it may be affected with long-term fiber maturation, growth factor supplementation, and mechanical stimulation.

Within 24 h of development, the cells became highly aligned and organized. Cellular organization was maintained following 72 h of growth, with no additional change in alignment from 24 h. Therefore, the organization of the cellular structure appears to be set within the first 24 h. This finding highlights our ability to provide early guidance cues for rapid cellular organization and alignment.

Despite the importance of cellular organization on tissue structure and function, there is a paucity of information on cellular organization in other ligament and tendon tissue engineering techniques. In a recent study, fibroblasts seeded in small intestine submucosa became more aligned following 5 days of cyclic stretch, compared to static controls.[33] Ma *et al.* showed that bone marrow stem cells, when cultured in a monolayer took up to 7 days to contract and form a tubular ligament-like structure.[34] While their study did not quantify cell alignment, typically confluent monolayers of adherent fibroblastic cells grown on 2D surfaces display swirl patterns of local alignment, and lack global alignment in a dominant direction. A recent approach to tendon engineering showed that, following 14 days in a scaffold-free,

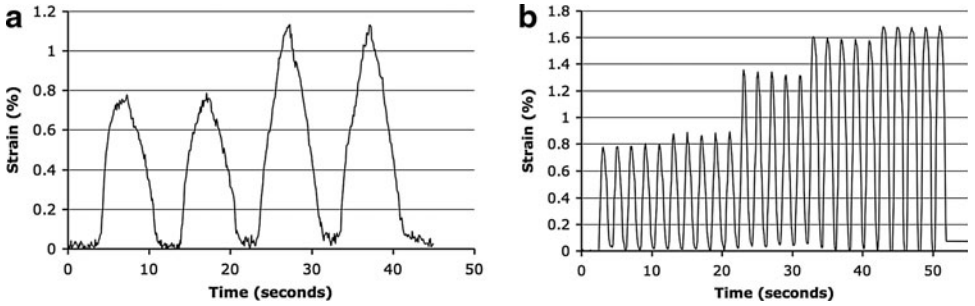


**FIG. 9.** Strain–time traces of dynamically strained growth channels determined from digital image correlation illustrating our ability to apply different amplitudes of cyclic strain at different frequencies. **(a)** Two unique strain magnitudes (two cycles each) applied at a frequency of 0.1 Hz, and **(b)** five unique strain magnitudes (five cycles each) at 0.5 Hz, show the modified Flexcell Tissue Train plates can apply specific amplitudes of dynamic strain with precise frequency resolution to the developing cellular fibers in the growth channels.

Table 1. Quantified Peak Strain Experienced in the Growth Channel, Determined from Digital Image Correlation (Mean ± St Dev)

| *Frequency (Hz)* | *Specified peak strain (%)* | *Peak strain in growth channel (%)* |
|---|---|---|
| 0.1 | 0.7 | 0.79 ± 0.1 |
| | 1.0 | 1.22 ± 0.13 |
| 0.5 | 0.7 | 0.77 ± 0.12 |
| | 0.75 | 0.83 ± 0.12 |
| | 1.0 | 1.21 ± 0.17 |
| | 1.5 | 1.49 ± 0.21 |
| | 2.0 | 1.6 ± 0.21 |

roller-tube culture, tendon fibroblasts appeared to be longitudinally aligned, but again organization was not quantified.[8] In addition to organization, cellular alignment may play a role in stem cell fate decisions, as human fetal tendon stem/progenitor cells exhibited enhanced scleraxis (a tendon-specific transcription factor) gene expression and collagen synthesis when cultured on aligned poly (L-lactic) acid nanofiber scaffolds, compared to unaligned scaffolds.[35] Rapid (~24 h) alignment of self-assembled cellular fibers may help guide cell fate decisions in addition to providing a foundation for accelerated tissue formation and maturation through the subsequent synthesis of an organized and aligned structural collagen matrix.

Application of cyclic tensile strain to the cellular fibers presented a unique challenge. To our knowledge, no other cellular assembly-based tendon or ligament tissue engineering technique has applied cyclic tensile strain to developing tissues *in vitro*, perhaps due to the complexities of a gripping and mechanically loading tissue that initially consists entirely of cells. The modifications to the Tissue Train plates (loading pins) and the incorporation of the collagen sponge anchor points into the ends of the growth channels allowed dynamic mechanical stimuli to be applied to the cellular fibers during development. By applying a well-characterized cyclic uniaxial tensile strain directly to the growth channels, dynamic mechanical stimulation can be applied early in fiber development (at 24 h), without the potential for damage or disruption that would occur if the fibers needed to be removed and grown in a separate bioreactor. Cellular fibers subjected to cyclic strains during development had a significantly increased maximum force and corresponding displacement, as well as nearly doubled linear-region stiffness, compared to static tension controls. Although no initial 3D scaffold was incorporated within the cellular fibers, the increase in linear-region stiffness and maximum load at failure with application of cyclic strain is consistent with the enhanced mechanical properties demonstrated in other tissue engineering techniques using mechanically stimulated, cell-seeded scaffolds.[36–39] This similar response to cyclic tensile strain suggests that (1) cells that form the fibers—independent of an initial 3D biomaterial scaffold—are capable of modifying the structure's mechanical properties, and (2) that cyclic strain may be a mechanism for tuning fiber properties to create mechanically matched soft tissue replacements.

Table 2. Mechanical Properties of Cellular Fibers (Mean ± St Dev)

| *Condition* | *Maximum force (mN)* | *Displacement at maximum force (mm)* | *Linear stiffness (mN/mm)* |
|---|---|---|---|
| Static | 0.04 ± 0.01 | 0.52 ± 0.17 | 0.1 ± 0.03 |
| Cyclic | 0.07 ± 0.02[a] | 0.84 ± 0.17[b] | 0.18 ± 0.07[c] |

[a]Significantly different from static, $p = 0.017$.
[b]Significantly different from static, $p = 0.012$.
[c]Nearly significantly different from static, $p = 0.06$.

These engineered cellular fibers, on the scale of primary single-tendon fibers,[40] may lay the foundation for the future creation of patient-specific, autologous cell-based soft tissue replacements. Within this tissue engineering approach, individual cellular fibers may be mechanically tuned, then bundled together to create entire tissue replacements, with fiber-level continuity and architectural fidelity.

In addition to laying the foundation for musculoskeletal soft tissue engineering, this approach may also offer an *in vitro* model system for studying early embryonic tissue development. The lack of an initial 3D biomaterial scaffold, and the resulting 3D cellular fiber structure, presents a unique opportunity to study how embryonic development-inspired factors affect cellular matrix synthesis and tissue formation. Utilizing this *in vitro* platform, we will investigate the biophysical stimuli (mechanical loading and soluble factors) involved in embryonic development. Cell types with either multipotent capacity or tendon-specific formation potential will be explored, such as mesenchymal stem cells,[41–43] tendon stem/progenitor cells,[44,45] and embryonic chick tendon progenitor cells.[46] Future tissue engineering studies will compare tissue formation between terminally differentiated (e.g., human dermal fibroblasts) and these multipotent progenitor cells. The influence of dynamic mechanical strain parameters (e.g., magnitude of strain, frequency of cyclic loading, and duration) and embryonic-inspired growth factors (e.g., growth factors specific to tenogenesis include the transforming growth factor-β3,[23] fibroblast growth factor [FGF4],[47] and FGF8[48]) on the resulting matrix synthesis and fiber biomechanics will be explored. This cellular, single-fiber tissue engineering approach has captured some key aspects of early embryonic tendon development and may provide unique insights into the functions and mechanisms of embryonic factors, which can then be translated to guide soft tissue engineering and regenerative medicine strategies.

## Acknowledgments

The authors would like to thank the Kensey Nash Corporation for the generous donation of the fibrous collagen sponge pads, as well as Scott Varney and Livingston Van De Water, PhD, of Albany Medical College for their assistance and expertise with immunocytochemistry. The authors would also like to thank Douglas M. Swank, PhD, and George E. Plopper, PhD, of Rensselaer Polytechnic Institute for the generous use of their equipment.

The National Science Foundation CBET CAREER 0954990 awarded to David T. Corr supported this study.

## Disclosure Statement

No competing financial interests exist.

## References


1. Provenzano, P.P., and Vanderby, R., Jr. Collagen fibril morphology and organization: implications for force transmission in ligament and tendon. Matrix Biol **25,** 71, 2006.
2. Butler, D.L., Juncosa, N., and Dressler, M.R. Functional efficacy of tendon repair processes. Annu Rev Biomed Eng **6,** 303, 2004.
3. Cohen, S., Leschansky, L., Zussman, E., Burman, M., Srouji, S., Abramov, N., and Itskovitz-Eldor, J. Repair of full-thickness tendon injury using connective tissue progenitors efficiently derived from human embryonic stem cells and fetal tissues. Tissue Eng Part A **16,** 3119, 2010.
4. Calve, S., Lytle, I.F., Grosh, K., Brown, D.L., and Arruda, E.M. Implantation increases tensile strength and collagen content of self-assembled tendon constructs. J Appl Physiol **108,** 875, 2010.
5. Calve, S., Dennis, R.G., Kosnik, P.E., 2nd, Baar, K., Grosh, K., and Arruda, E.M. Engineering of functional tendon. Tissue Eng **10,** 755, 2004.
6. Larkin, L.M., Calve, S., Kostrominova, T.Y., and Arruda, E.M. Structure and functional evaluation of tendon-skeletal muscle constructs engineered *in vitro*. Tissue Eng **12,** 3149, 2006.
7. Hairfield-Stein, M., England, C., Paek, H.J., Gilbraith, K.B., Dennis, R., Boland, E., and Kosnik, P. Development of self-assembled, tissue-engineered ligament from bone marrow stromal cells. Tissue Eng **13,** 703, 2007.
8. de Wreede, R., and Ralphs, J.R. Deposition of collagenous matrices by tendon fibroblasts *in vitro*: a comparison of fibroblast behavior in pellet cultures and a novel three-dimensional long-term scaffoldless culture system. Tissue Eng Part A **15,** 2707, 2009.
9. Patz, T.M., Doraiswamy, A., Narayan, R.J., Modi, R., and Chrisey, D.B. Two-dimensional differential adherence and alignment of C2C12 myoblasts. Mater Sci Eng **123,** 242, 2005.
10. Vukicevic, S., Kleinman, H.K., Luyten, F.P., Roberts, A.B., Roche, N.S., and Reddi, A.H. Identification of multiple active growth factors in basement membrane Matrigel suggests caution in interpretation of cellular activity related to extracellular matrix components. Exp Cell Res **202,** 1, 1992.
11. Kleinman, H.K., Mcgarvey, M.L., Liotta, L.A., Robey, P.G., Tryggvason, K., and Martin, G.R. Isolation and characterization of type-Iv procollagen, laminin, and heparan-sulfate proteoglycan from the Ehs sarcoma. Biochemistry **21,** 6188, 1982.
12. Liu, C.F., Aschbacher-Smith, L., Barthelery, N.J., Dyment, N., Butler, D., and Wylie, C. What we should know before using tissue engineering techniques to repair injured tendons: a developmental biology perspective. Tissue Eng Part B Rev **17,** 165, 2011.
13. Thomopoulos, S., Genin, G.M., and Galatz, L.M. The development and morphogenesis of the tendon-to-bone insertion—what development can teach us about healing. J Musculoskelet Neuronal Interact **10,** 35, 2010.
14. Brown, J.P., Lind, R.M., Burzesi, A.F., and Kuo, C.K. Elastogenic protein expression of a highly elastic murine spinal ligament: the ligamentum flavum. PLoS One **7,** e38475, 2012.
15. Oryan, A., and Shoushtari, A.H. Histology and ultrastructure of the developing superficial digital flexor tendon in rabbits. Anat Histol Embryol **37,** 134, 2008.
16. Ansorge, H.L., Adams, S., Birk, D.E., and Soslowsky, L.J. Mechanical, compositional, and structural properties of the post-natal mouse Achilles tendon. Ann Biomed Eng **39,** 1904, 2011.
17. Chaplin, D.M., and Greenlee, T.K., Jr. The development of human digital tendons. J Anat **120,** 253, 1975.
18. McNeilly, C.M., Banes, A.J., Benjamin, M., and Ralphs, J.R. Tendon cells *in vivo* form a three dimensional network of cell processes linked by gap junctions. J Anat **189 (Pt 3),** 593, 1996.
19. Richardson, S.H., Starborg, T., Lu, Y., Humphries, S.M., Meadows, R.S., and Kadler, K.E. Tendon development requires regulation of cell condensation and cell shape via cadherin-11-mediated cell-cell junctions. Mol Cell Biol **27,** 6218, 2007.
20. Kiener, H.P., and Brenner, M.B. Building the synovium: cadherin-11 mediates fibroblast-like synoviocyte cell-to-cell adhesion. Arthritis Res Ther **7,** 49, 2005.
21. Suzue, T., and Shinoda, Y. Highly reproducible spatiotemporal patterns of mammalian embryonic movements at the developmental stage of the earliest spontaneous motility. Eur J Neurosci **11,** 2697, 1999.
22. Wu, K.C., Streicher, J., Lee, M.L., Hall, B.K., and Muller, G.B. Role of motility in embryonic development I: embryo movements and amnion contractions in the chick and the influence of illumination. J Exp Zool **291,** 186, 2001.
23. Kuo, C.K., Petersen, B.C., and Tuan, R.S. Spatiotemporal protein distribution of TGF-betas, their receptors, and extracellular matrix molecules during embryonic tendon development. Dev Dyn **237,** 1477, 2008.
24. Connell, D., Datir, A., Alyas, F., and Curtis, M. Treatment of lateral epicondylitis using skin-derived tenocyte-like cells. Br J Sports Med **43,** 293, 2009.
25. Deng, D., Liu, W., Xu, F., Yang, Y., Zhou, G., Zhang, W.J., Cui, L., and Cao, Y. Engineering human neo-tendon tissue *in vitro* with human dermal fibroblasts under static mechanical strain. Biomaterials **30,** 6724, 2009.
26. Clarke, A.W., Alyas, F., Morris, T., Robertson, C.J., Bell, J., and Connell, D.A. Skin-derived tenocyte-like cells for the treatment of patellar tendinopathy. Am J Sports Med **39,** 614, 2011.
27. Ng, C.P., and Swartz, M.A. Mechanisms of interstitial flow-induced remodeling of fibroblast-collagen cultures. Ann Biomed Eng **34,** 446, 2006.
28. Glawe, J.D., Hill, J.B., Mills, D.K., and McShane, M.J. Influence of channel width on alignment of smooth muscle cells by high-aspect-ratio microfabricated elastomeric cell culture scaffolds. J Biomed Mater Res A **75,** 106, 2005.
29. Ng, C.P., Hinz, B., and Swartz, M.A. Interstitial fluid flow induces myofibroblast differentiation and collagen alignment *in vitro*. J Cell Sci **118,** 4731, 2005.
30. Palmer, B.M., and Bizios, R. Quantitative characterization of vascular endothelial cell morphology and orientation using Fourier transform analysis. J Biomech Eng **119,** 159, 1997.
31. Wang, J.H. Mechanobiology of tendon. J Biomech **39,** 1563, 2006.
32. Eldred, C.C., Simeonov, D.R., Koppes, R.A., Yang, C., Corr, D.T., and Swank, D.M. The mechanical properties of Drosophila jump muscle expressing wild-type and embryonic Myosin isoforms. Biophys J **98,** 1218, 2010.
33. Nguyen, T.D., Liang, R., Woo, S.L.Y., Burton, S.D., Wu, C.F., Almarza, A., Sacks, M.S., and Abramowitch, S. Effects of cell seeding and cyclic stretch on the fiber remodeling in an extracellular matrix-derived bioscaffold. Tissue Eng Part A **15,** 957, 2009.
34. Ma, J., Goble, K., Smietana, M., Kostrominova, T., Larkin, L., and Arruda, E.M. Morphological and functional characteristics of three-dimensional engineered bone-ligament-bone

constructs following implantation. J Biomech Eng **131,** 101017, 2009.
35. Yin, Z., Chen, X., Chen, J.L., Shen, W.L., Nguyen, T.M.H., Gao, L., and Ouyang, H.W. The regulation of tendon stem cell differentiation by the alignment of nanofibers. Biomaterials **31,** 2163, 2010.
36. Nirmalanandhan, V.S., Shearn, J.T., Juncosa-Melvin, N., Rao, M., Gooch, C., Jain, A., Bradica, G., and Butler, D.L. Improving linear stiffness of the cell-seeded collagen sponge constructs by varying the components of the mechanical stimulus. Tissue Eng Part A **14,** 1883, 2008.
37. Shearn, J.T., Juncosa-Melvin, N., Boivin, G.P., Galloway, M.T., Goodwin, W., Gooch, C., Dunn, M.G., and Butler, D.L. Mechanical stimulation of tendon tissue engineered constructs: effects on construct stiffness, repair biomechanics, and their correlation. J Biomech Eng **129,** 848, 2007.
38. Garvin, J., Qi, J., Maloney, M., and Banes, A.J. Novel system for engineering bioartificial tendons and application of mechanical load. Tissue Eng **9,** 967, 2003.
39. Issa, R.I., Engebretson, B., Rustom, L., McFetridge, P.S., and Sikavitsas, V.I. The effect of cell seeding density on the cellular and mechanical properties of a mechanostimulated tissue-engineered tendon. Tissue Eng Part A **17,** 1479, 2011.
40. Kannus, P. Structure of the tendon connective tissue. Scand J Med Sci Sports **10,** 312, 2000.
41. Kuo, C.K., and Tuan, R.S. Mechanoactive tenogenic differentiation of human mesenchymal stem cells. Tissue Eng Part A **14,** 1615, 2008.
42. Juncosa-Melvin, N., Shearn, J.T., Boivin, G.P., Gooch, C., Galloway, M.T., West, J.R., Nirmalanandhan, V.S., Bradica, G., and Butler, D.L. Effects of mechanical stimulation on the biomechanics and histology of stem cell-collagen sponge constructs for rabbit patellar tendon repair. Tissue Eng **12,** 2291, 2006.
43. Lee, J.Y., Zhou, Z., Taub, P.J., Ramcharan, M., Li, Y., Akinbiyi, T., Maharam, E.R., Leong, D.J., Laudier, D.M., Ruike, T., Torina, P.J., Zaidi, M., Majeska, R.J., Schaffler, M.B., Flatow, E.L., and Sun, H.B. BMP-12 treatment of adult mesenchymal stem cells *in vitro* augments tendon-like tissue formation and defect repair *in vivo*. PLoS One **6,** e17531, 2011.
44. Zhang, J., Li, B., and Wang, J.H.C. The role of engineered tendon matrix in the stemness of tendon stem cells *in vitro* and the promotion of tendon-like tissue formation *in vivo*. Biomaterials **32,** 6972, 2011.
45. Bi, Y., Ehirchiou, D., Kilts, T.M., Inkson, C.A., Embree, M.C., Sonoyama, W., Li, L., Leet, A.I., Seo, B.-M., Zhang, L., Shi, S., and Young, M.F. Identification of tendon stem/progenitor cells and the role of the extracellular matrix in their niche. Nat Med **13,** 1219, 2007.
46. Kapacce, Z., Richardson, S.H., Lu, Y.H., Starborg, T., Holmes, D.F., Baar, K., and Kadler, K.E. Tension is required for fibripositor formation. Matrix Biol **27,** 371, 2008.
47. Edom-Vovard, F., Schuler, B., Bonnin, M.A., Teillet, M.A., and Duprez, D. Fgf4 positively regulates scleraxis and tenascin expression in chick limb tendons. Dev Biol **247,** 351, 2002.
48. Edom-Vovard, F., Bonnin, M., and Duprez, D. Fgf8 transcripts are located in tendons during embryonic chick limb development. Mech Dev **108,** 203, 2001.

Address correspondence to:
*David T. Corr, PhD*
*Biomedical Engineering Department*
*Jonsson Engineering Center*
*Room 7042*
*110 8th Street*
*Troy, New York 12180-3590*

*E-mail:* corrd@rpi.edu

*Received: May 23, 2012*
*Accepted: December 07, 2012*
*Online Publication Date: January 23, 2013*